



Preparation and electrochemistry properties of trifunctional 1,9-dithiophenalenylium salt and its neutral radical with benzene spacer



Guangrui He^a, Yanhui Hou^b, Dong Sui^a, Xiangjian Wan^a, Guankui Long^a, Peng Yun^c,
Ao Yu^c, Mingtao Zhang^c, Yongsheng Chen^{a,*}

^aKey Laboratory for Functional Polymer Materials and Centre for Nanoscale Science and Technology, Institute of Polymer Chemistry, College of Chemistry, Nankai University, Tianjin 300071, China

^bSchool of Materials Science and Engineering, Tianjin Polytechnic University, Tianjin 300160, China

^cCentral Laboratory, College of Chemistry, Nankai University, Tianjin 300071, China

ARTICLE INFO

Article history:

Received 27 February 2013

Received in revised form 18 May 2013

Accepted 27 May 2013

Available online 11 June 2013

Keywords:

Radical

Phenalenyl

Spin density distribution

Electrochemistry

ABSTRACT

A trifunctional 1,9-dithiophenalenylium salt with benzene spacer has been prepared as the precursor for a phenalenyl-based high spin radical. Electrochemical studies show that this salt undergoes two three-electron reduction steps and generate its corresponding neutral radical, which has been studied by quantum chemical calculations. The investigation of the spin density distribution of the radical revealed that the spin and electronic properties of molecules based on phenalenyl systems are strongly influenced by intramolecular topology connection.

© 2013 Elsevier Ltd. All rights reserved.

1. Introduction

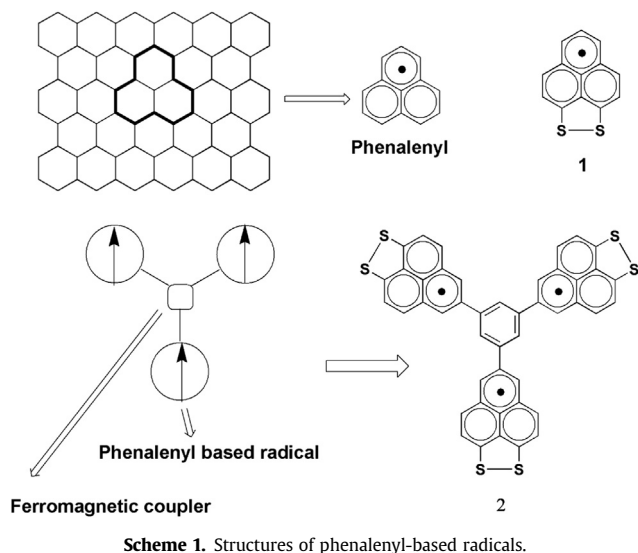
Cutting of graphene in a triangular manner will lead to a series of non-Kekule polycyclic hydrocarbons with one or more unpaired electrons, which can be termed as ‘open-shell graphene fragments’ and are very interesting both theoretically and experimentally [1,2]. The smallest member in this family, the phenalenyl (PLY) radical, is especially attractive due to its high symmetry ($D3h$) and an accessible triad of oxidation states: the diamagnetic cation, the paramagnetic radical, and the diamagnetic anion are all stable [3,4]. Quite some of these PLY based stable radical organic molecules with this or similar structures have been synthesized and characterized elegantly by Haddon [5–13] and other groups [14–19]. Among all these molecules, 1,9-dithiophenalenyl radical **1** is unique. In this molecule crystal, while localized C–C σ -dimerization was suppressed, a planer structure and p -electron orbital overlap between the adjacent PLY molecules was maintained, due to the enhanced delocalization provided by the peripheral heteroatoms [10,20,21].

With certain topology structure, several mono- [9,11,14,15,22] bis- [23–29], and tris- [7,13] phenalenyl-based radicals have been synthesized and crystallized (Scheme 1), in the pursuit of (PLY)-based neutral radical molecular conductors and nonlinear optics (NLO) materials [29,30], and so on. In these phenalenyl (PLY) radical based molecules, with different topological connection, unpaired electrons or partially unpaired electrons will display open-shell radical character. This can lead to special features in electronic structures, magnetic properties, optical properties and crystalline packing, which endow them with great potential as a new generation of materials [1].

Recently, theoretical and experimental studies have reported the emergence of ferromagnetism in graphene and graphite materials, even at room temperature [31–35]. Much more through study were needed in the molecular level of organic material room temperature ferromagnetism [36–38]. Being the simplest building block for graphene fragments with nonzero net spin, PLY based high spin organic molecules are expected to be the spin module for forming a magnetically active bulk material and give some implication for the room temperature ferromagnetism in graphene [1,30,35].

Herein, our targeted molecule is the PLY based triradical compound **2** (Scheme 1) with $D3h$ symmetry. In this molecule, the 1,9-

* Corresponding author. Tel.: +86 022 23500693; fax: +86 022 23499992; e-mail address: yschen99@nankai.edu.cn (Y. Chen).

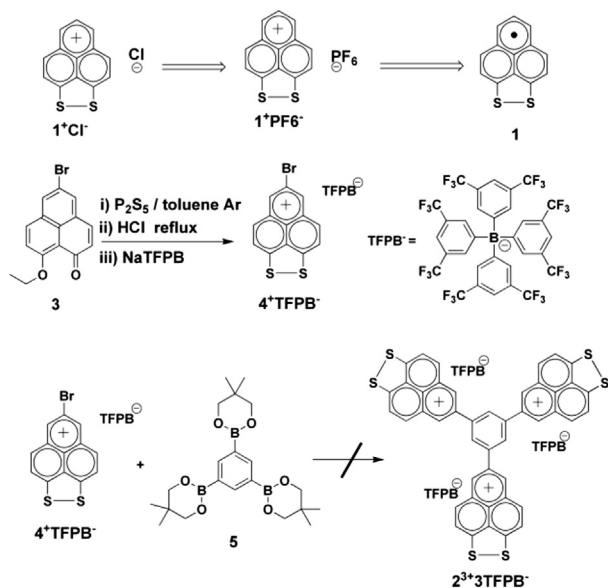


dithiophenalenyl system as the radical unit and the 1,3,5-substituted benzene core was used as a ferromagnetic coupler [39,40].

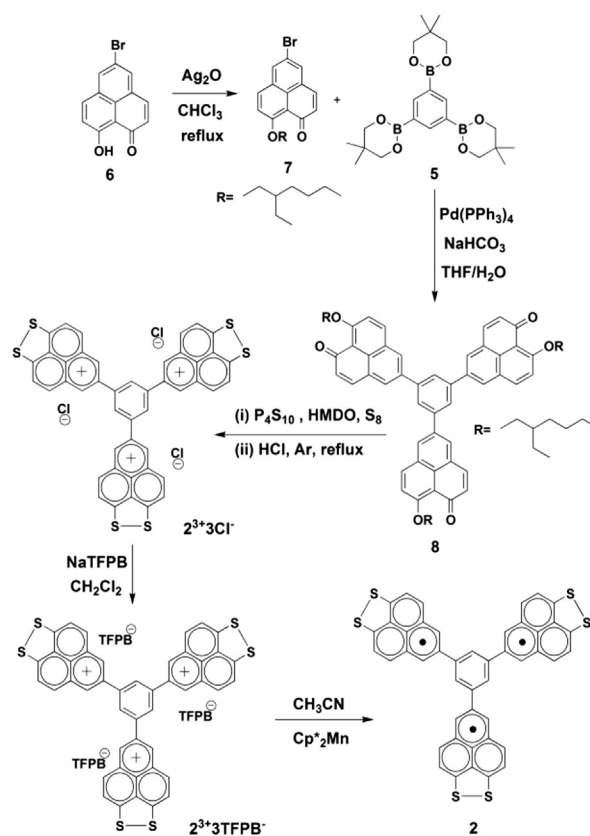
2. Results and discussion

2.1. Synthesis of soluble precursor salt of trifunctional radical

From Haddon's work, it can be seen that the salt 1^+Cl^- is the key intermediate for radical **1** [41]. There are quite some challenges associated with the synthesis of the key precursor $2^{3+}3\text{Cl}^-$, partially due to its low solubility. At first, we tried the strategy through coupling reaction between the monomer salt 4^+TFPB^- and 1,3,2-(3,5-bis(5,5-dimethyl-1,3,2-dioxaborinan-2-yl)phenyl)-5,5-dimethyl-1,3,2-dioxaborinane **5** as described in Scheme 2, similar to our previous synthesis route of PLY radical [42]. However, we found that the product of coupling reaction are difficult to purify and characterize, for the salt 4^+TFPB^- is not stable in silica gel. In addition, recrystallization from different solvent also failed to obtain pure product.



Finally, we tried the following route to synthesize the key precursor $2^{3+}3\text{Cl}^-$ and $2^{3+}3\text{TFPB}^-$ as shown in Scheme 3.



The compound 5,5',5''-(1,3,5-phenylene)tris[9-(2-ethylhexoxy)-1-oxophenalene] **8** was produced via Suzuki reaction between **5** and **7**. It is worth noting that the solvent of tetrahydrofuran (THF) mixed with water is rather important for the success of the coupling reaction. Note that the iso-octyl attached to **8** was used to improve the solubility of **8** and enable the following reaction to go through completely.

The synthesis of the salt $2^{3+}3\text{Cl}^-$ followed a procedure with a slight modification of Haddon's method [10]. Here, hexamethyldisiloxane (HMDO) and sublimed sulfur, combining with P_4S_{10} , were used to improve the yield [43]. The chloride salts are quite insoluble in most common organic solvent but are sparingly soluble in dichloromethane. In order to achieve the required solubility for the 2^{3+} (Scheme 3), $2^{3+}3\text{TFPB}^-$ was obtained by the anion exchange of $2^{3+}3\text{Cl}^-$ with sodium tetrakis[3,5-bis(trifluoromethyl)phenyl] borate (NaTFPB) in dry dichloromethane. $2^{3+}3\text{TFPB}^-$ is not stable on silica gel, recrystallization is the only way to purify the TFPB salt. Fortunately, we found that recrystallization from cold dichloromethane can remove the excess NaTFPB and other impurity. As expected, $2^{3+}3\text{TFPB}^-$ has an excellent solubility in many common organic solvents, such as acetone, methanol, dichloromethane, THF, dichlorobenzene, and so on (Table S1). $2^{3+}3\text{TFPB}^-$ was characterized and confirmed by ^1H NMR (Fig. 1), ^{13}C NMR and High Resolution Mass Spectrum (Figs. S3, S4, S10, S14).

Combined with Refs. [41,43–45] and experiment result, the reaction mechanism of the formation of the key salt was proposed as shown in Scheme S2.

In addition, we found that the solubility of the salt 2^{3+} can be tuned easily by varying different counter ions (Table S1). $2^{3+}3\text{PF}_6^-$, $2^{3+}3\text{BPh}_4^-$, $2^{3+}3\text{SbF}_6^-$ salts can be obtained through anion exchange

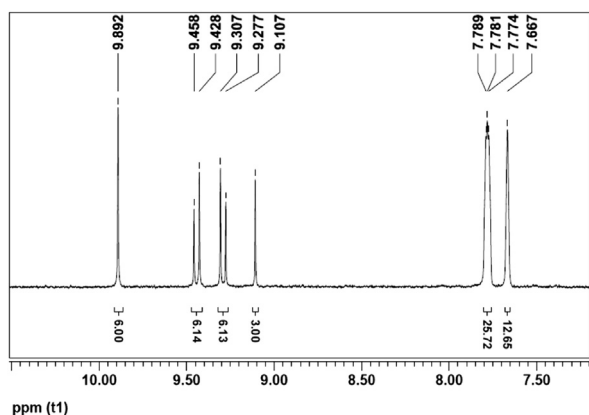


Fig. 1. ^1H NMR of $2^{3+}3\text{TFPB}^-$ in CD_3COCD_3 .

from $2^{3+}3\text{TFPB}^-$. The different solubility of these salts served as the driving force of the anion metathesis.

2.2. Absorption spectra of the precursor salt

The UV–vis absorption spectra of $2^{3+}3\text{TFPB}^-$, together with compounds **8**, **7** and **3** for comparison, in diluted dichloromethane solution with a concentration of 10^{-5} mol L^{-1} and $2^{3+}3\text{TFPB}^-$ film drop onto SiO_2 are shown in Fig. 2.

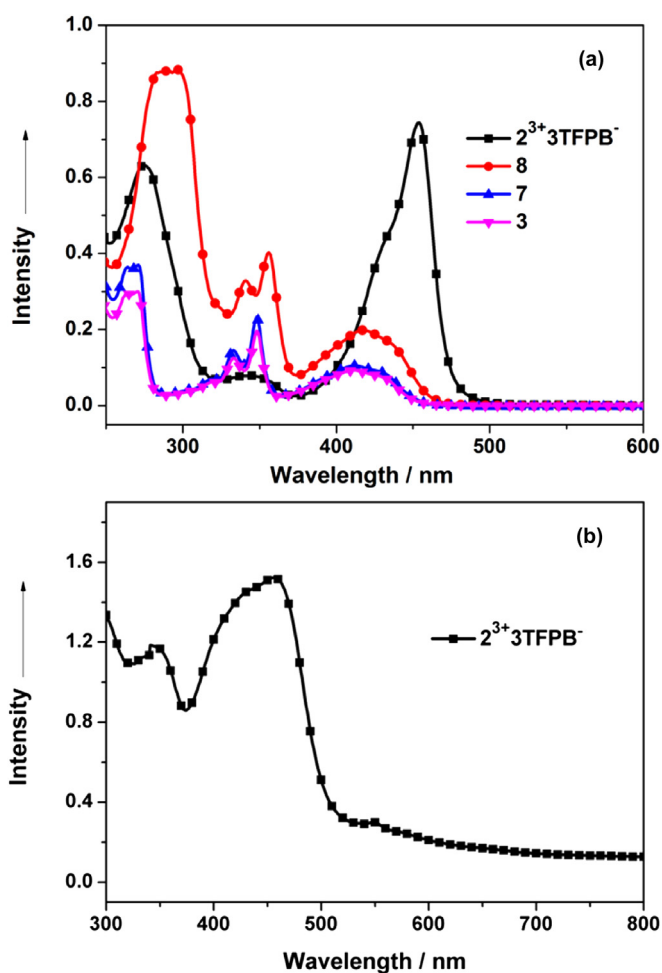


Fig. 2. (a) UV–vis of $2^{3+}3\text{TFPB}^-$ and other molecules in CH_2Cl_2 with a concentration of 1×10^{-5} M (b) UV–vis of $2^{3+}3\text{TFPB}^-$ film dropped onto SiO_2 .

Compared with the absorption peaks at 419 nm of **8** solution, as shown in Fig. 2 and Table S2, $2^{3+}3\text{TFPB}^-$ have a red-shift of about 34 nm, with a more strong absorption peak at 453 nm. This means that $2^{3+}3\text{TFPB}^-$ have a larger delocalized π electron system.

As shown in Fig. 3, the onset absorption of $2^{3+}3\text{TFPB}^-$ film is 540 nm, thus the optical bandgap of $2^{3+}3\text{TFPB}^-$ is 2.3 eV.

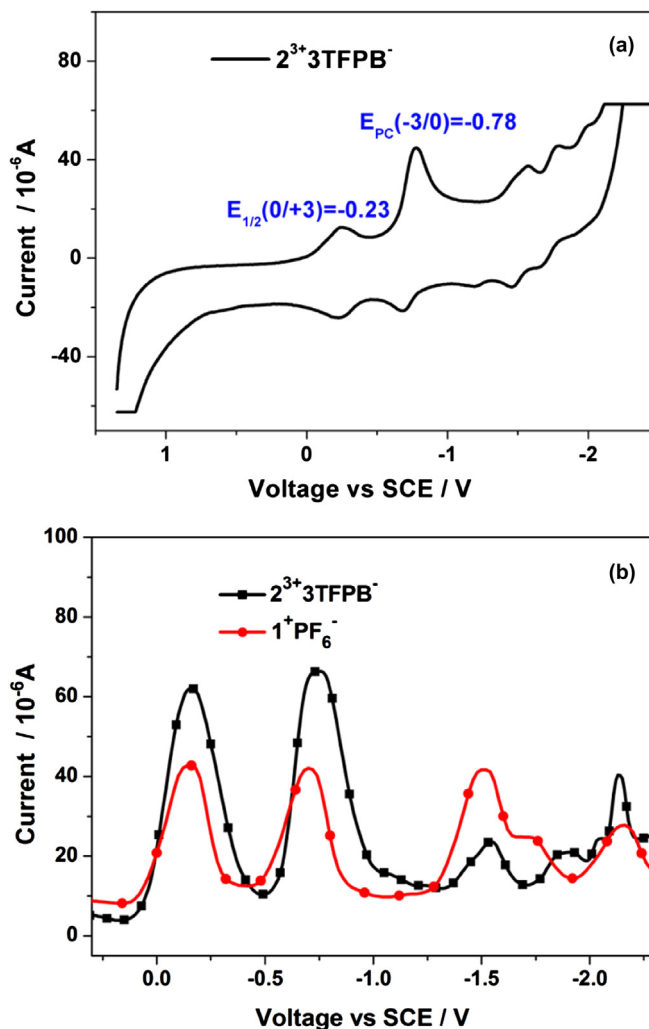


Fig. 3. (a) Cyclic voltammogram for $2^{3+}3\text{TFPB}^-$ in DMF, 0.1 M $n\text{-Bu}_4\text{N}^+\text{PF}_6^-$ supporting electrolyte, scan rate 100 mV/S. (b) Differential pulse voltammetry (DPV) for $2^{3+}3\text{TFPB}^-$ and 1^+PF_6^- in DMF, 0.1 M $n\text{-Bu}_4\text{N}^+\text{PF}_6^-$ supporting electrolyte.

2.3. Electrochemical properties of the precursor salt

The electrochemical behavior of $2^{3+}3\text{TFPB}^-$ was studied by cyclic voltammetry (CV) and differential pulse voltammetry (DPV) (Fig. 3), and the results are summarized in Table 1 together with the corresponding data reported for some related compounds (Scheme 4).

As shown in Fig. 3 and Table 1, the first and second reduction potentials of the salt $2^{3+}3\text{TFPB}^-$ occur at almost the same potentials as that required for the reduction of 1^+OTf^- [10]. Combined with the calculated result in the following, we proposed that the cyclic voltammetry of $2^{3+}3\text{TFPB}^-$ in degassed dry DMF solutions shows two ‘three-electron redox waves’: a reversible ‘0/+3 wave’ with $E_{1/2}$ values of -0.23 V (vs SCE) and a quasi-reversible waves corresponding to the ‘–3/0 couple’ with E_{PC} values of -0.78 V, the strong cathodic wave of the latter suggesting electroreduction of material coating the electrode. As shown in Fig. 3a, the first ‘three-electron redox wave’, in detail, should be the superposition of the

Table 1
Solution redox potential for PLY based molecules

Compounds	$E_{1/2}^{(1/2+)}$	$E_{1/2}^{(0/1+)}$	$E_{1/2}^{(1/2^0)}$	$E_{1/2}^{(2-/1-)}$
PLY ^a		0.7		-1.6
1 ^b		-0.23	-0.9	-1.53
9 ^c	0.83	0.39	-0.80	-1.35
10 ^d		-0.73	-1.12	
11 ^e		-0.39	-1.10	
1 (DPV)		-0.19	-0.72	-1.52
2 (CV)		$E_{1/2}^{(0/3+)}$ -0.23	$E_{pc}^{(3-/0)}$ -0.78	$E_{pc}^{(6-/3-)}$ -1.58
2 (DPV)		-0.20	-0.74	-1.54

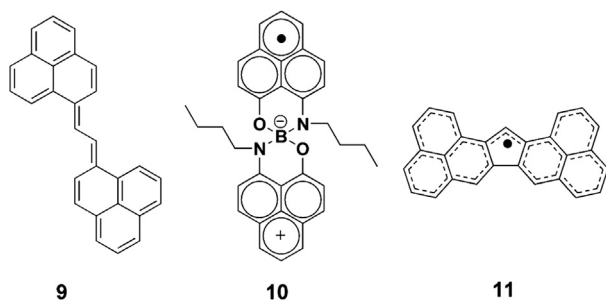
^a Literature [41] (in acetonitrile, referenced to SCE, 0.1 M (*n*-Bu)₄NBF₄, rt).

^b Literature [10] (in acetonitrile, referenced to SCE, 0.1 M (*n*-Bu)₄NBF₄, rt).

^c Literature [18] (in DMF, referenced to SCE, with 0.1 M Et₄NClO₄, -50 °C).

^d Literature [23] (in acetonitrile, referenced to SCE via internal ferrocene, rt).

^e Literature [6] (in CH₂Cl₂, referenced to vs Fc/Fc, 0.1 M (ⁿBu)₄NClO₄, rt).



Scheme 4. Some PLY based molecules with typical topological structure.

three one-electron steps: $E_{pc}(+2/+3, +1/+2$ and $0/+1)$. In similar, the second ‘three-electron redox wave’ corresponds to the series of overlapping one-electron waves of $E_{pc}(-1/0, -2/-1, -3/-2)$.

Differential pulse voltammetry (DPV) of compounds $2^{3+}3TFPB^-$ and 1^+PF6^- was performed to give clear redox potentials. From Table 1 and Fig. 3b, we can see that $2^{3+}3TFPB^-$ shows a series of redox peaks at -0.20 V, -0.74 V, and -1.54 V, similar to that of 1^+PF6^- (-0.19 V, -0.72 V, and -1.52 V).

Furthermore, additional reduction waves can also be seen in the CV curves, similar to that in the case of 1^+OTf^- . On the separation of the two E_{pc} values (-1/0 and 0/+1), we estimate a disproportionation potential of -0.55 V, similar to that of single radical **1** (-0.57 V) [10].

2.4. Reduction of the precursor salt

According to the redox potentials of the salts $2^{3+}3TFPB^-$ and several common reductants (shown in Table S3), bis-(pentamethylcyclopentadienyl)manganese(II) Cp*₂Mn was chosen as the reductant because its oxidation potential ($E_{1/2} = -0.56$ V vs SCE) [10] falls between the first $E_{pc}(0/+3)$ and the second $E_{pc}(-3/0)$ of $2^{3+}3TFPB^-$. A clear ESR spectrum was obtained for the solid product (Fig. 4), which indicates the targeted neutral radical was generated. Due to the insolubility of this radical, the ESR spectrum only gives a very broad peak with the *g*-factor of 2.0034, consistent with other *g* values of the PLY radical family [10]. But its insolubility has prevented a full investigation of this neutral radical.

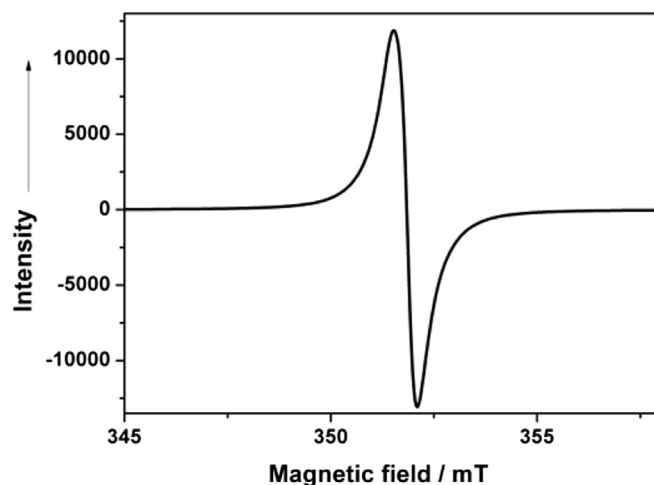


Fig. 4. ESR spectrum of radical **2** as a powder sample, recorded at 293 K. Frequency is 9.849 GHz.

2.5. Quantum calculations

The CV result of $2^{3+}3TFPB^-$ can be traced back to the electronic structure of the radical **2**, which were generated by combining the molecular orbitals (MOs) of its three parent radical **1** and the benzene spacer [46]. As illustrated in Fig 5 and listed in Table S4, the frontier orbitals of **2**: singly occupied molecule orbital (SOMO), (SOMO-1), and (SOMO-2) are nearly degenerated orbitals having the same energy, meaning lack of electronic coupling in such system. Thus, the three PLY moiety appear to behave as noninteracting equivalent redox centers and the two ‘three-electron reduction’ can be seen.

For further understanding, we investigated the spin density distributions of the radicals **1**, **2** and the unsubstituted PLY (Fig. 6), which were performed by DFT calculation (PBE1PBE/6-31g*), and the frequency analysis was followed to assure that the optimized structures were stable states [46]. For unsubstituted PLY and **1**, the α spin density are mainly distributed on the positions of C1, C3, C4, C6, C7, and C9, while little was distributed on C2, C5, and C8 positions, where are the nodes in the wave function of SOMO of PLY or **1**. Then, for the radical **2**, most of the spin density is populated on the PLY nucleus, and little amount of the spin densities are distributed on the benzene spacer, which is connected to the C5 (node) with little spin distribution. So most of the spin is still distributed on the PLY unit, probably due to the topological connection in the molecule as discussed below.

In fact, many examples have shown that the spin and electronic properties of molecules based on PLY systems are strongly influenced by intramolecular topology connection. As shown in Scheme 4, compounds **9** [18], **10** [23], and **11** [6] all have at least one spin rich position in PLY unit to be connected to the spacer or bridge unit. Thus, this type of connection could result in enhanced electronic coupling of the PLY units. As shown in Table 1, all these three compounds show distinct multistage one-electron redox waves.

The different connection makes radical **2** behaves very differently compared with compounds **9–11**. (i) For compound **9**, there are even π electrons (a double bond or a benzene) between the two PLY radical units with the active position (spin rich sites) connection. Thus, a closed-shell Kekule structure was formed, which is in resonance with the open-shell singlet biradical. These kind of molecules based materials have nonlinear optics (NLO) properties [2,18]. (ii) For **10** and **11**, there are odd π electrons (a ‘CH’ or ‘BO₂N₂’) between two PLY radicals with active carbon link and highly delocalized phenalenyl-based monoradicals were formed. In these molecules, the unpaired electron can delocalize over the whole

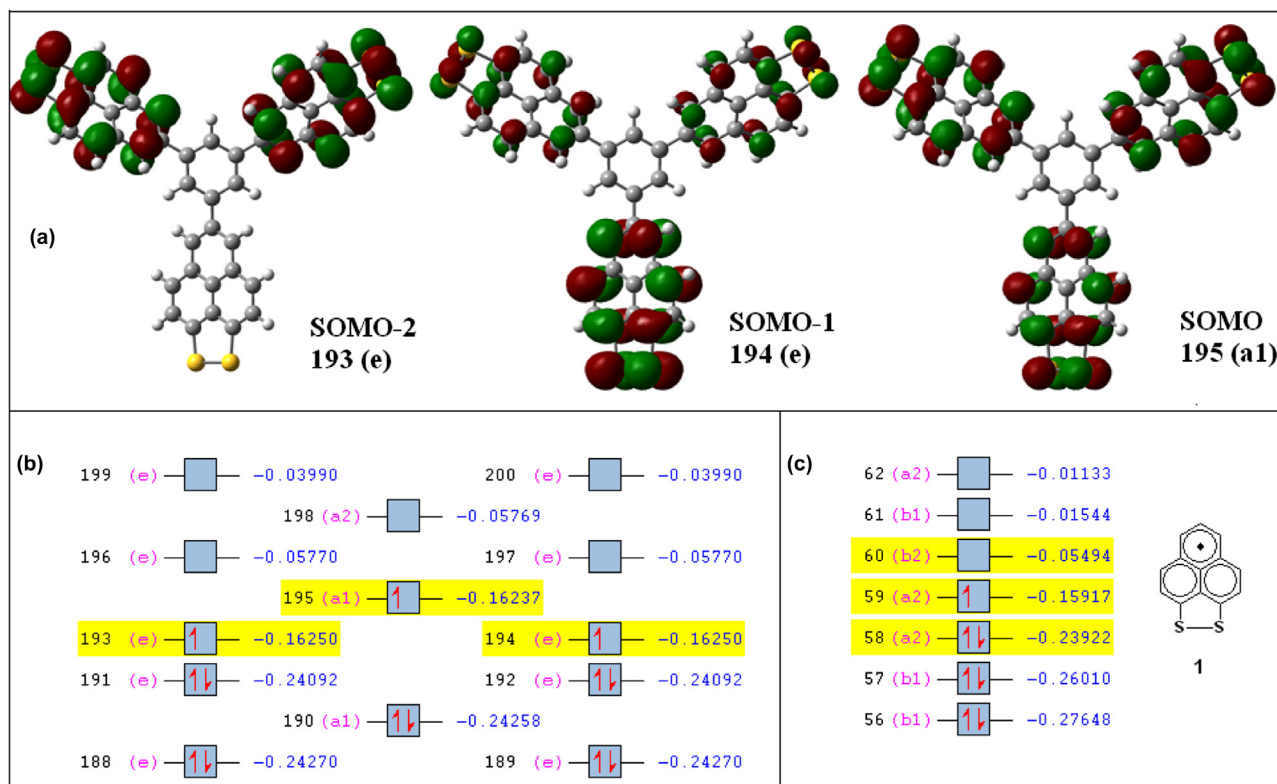


Fig. 5. (a). Calculated SOMO-2, SOMO-1, and SOMO of **2**; (b) some related MOs of **2**; (c) some related MOs of **1**. Energy unit: a.u.

molecule through the resonance of two canonical forms having a phenalenyl radical structure and a smaller disproportionation potential can always be found [7,12,13,23,26]. (iii) For radical **2**, with linkers only substitute at the unactive (nodal) carbons on PLY unit,

a three-independent PLY based triradical system is formed and the three unpaired electrons on the three PLY units are distributed in three (near) degenerate orbitals. The ground state of this molecule is also described as high spin system with multiple parallel spin.

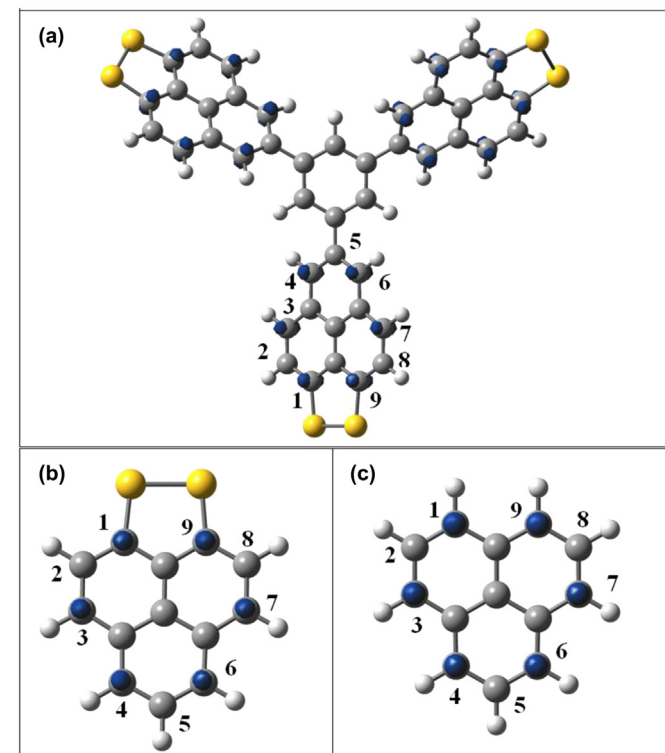


Fig. 6. Spin density map of **2** (a), **1** (b) and PLY (c) calculated with a PBE1PBE/6-31G(d) method. Blue and green surfaces represent α and β spin densities, drawn at 0.02 $e/a.u.^2$ level, respectively.

3. Conclusion

In summary, we have successfully synthesized a cationic tri-functional 1,9-dithiophenalenylium salt with a benzene spacer, $2^{3+}3TFPB^-$. The salt exhibited two ‘three-electron reduction waves’, which was explained by quantum chemical calculations and its topological connection structure. The investigation of the SOMO and spin density distribution of **2** revealed that the spin and electronic properties of molecules based on PLY systems are strongly influenced by intramolecular topology connection. In addition, the high stabilization of **2** with three-electron spinning parallel each other, opens the door to get PLY based stable radical with high spins. These results warrant a full investigation of the solid-state properties, such as crystal packing, magnetism and conductivity of this kind of molecules with proper alkyl substituent.

4. Experimental section

4.1. Reagents and instruments

Hexamethyldisiloxane (HMDO), Ag_2O , $NaHCO_3$, $Pd(PPh_3)_4$, bis-(pentamethylcyclopentadienyl)manganese(II) (Cp^*_2Mn) and P_4S_{10} were all commercial products and were used as received. 5-Bromo-9-hydroxy-1-oxophenylene (**6**) [47], sodium tetrakis[(3,5-trifluoromethyl)phenyl]borate ($NaTFPB$) [48], and 2-(3,5-bis(5,5-dimethyl-1,3,2-dioxaborinan-2-yl)phenyl)-5,5-dimethyl-1,3,2-dioxaborinane (**5**) [49] were prepared using procedures reported in the literature. All manipulations were carried out under a dry argon atmosphere using standard Schlenk techniques, and solvents

were purified by standard procedures. ^1H NMR spectra were recorded on a Bruker AC-300 spectrometer. ^{13}C NMR spectra were recorded on a Bruker AC-400 spectrometer. Chemical shifts were recorded in parts per million relative to the internal standard TMS. Mass spectra were recorded on a LCQ Advantage spectrometer with ESI resource. HRMS were recorded on a VG ZAB-HS mass spectrometer with MALDI resource. MALDI-TOF MS analysis was performed on a Bruker BIFLEX III mass spectrometer. UV–vis–NIR spectra were obtained using Bruker–Tensor 27 and JASCO-V570 spectrometers, respectively. Cyclic voltammetric measurement was performed on a LK98BII Microcomputer-based Electrochemical Analyzer, using a Pt wire electrode with $n\text{-Bu}_4\text{NPF}_6$ as the supporting electrolyte, with a SCE reference electrode. ESR studies were performed with a Bruker EMX-6/1 spectrometer on the loose packed powder.

4.2. Synthesis

The synthetic route of the **2** is shown in Schemes 2 and 3. The detailed synthetic procedures are as follows.

4.2.1. 5-Bromo-9-ethoxy-1-oxophenalene (3). 5-Bromo-9-hydroxy-1-oxophenalene (**6**) (5.48 g, 20 mmol), silver oxide (4.63 g, 20 mmol), and ethyl iodide (4.68 g, 30 mmol) were stirred in chloroform (50 mL). The mixture was held at reflux for 12 h, then cooled to room temperature and filtered. The filtrate was evaporated to dryness under reduced pressure and a yellow solid was left. Recrystallization from tetrahydrofuran gave a yellow needle solid (5.44 g, yield 90%). ^1H NMR (400 M, CDCl_3): δ 7.88 (d, $J=9.2$ Hz, 1H), 7.86 (s, 1H), 7.66 (s, 1H), 7.47 (d, $J=9.6$ Hz, 1H), 7.34 (d, $J=9.2$ Hz, 1H), 6.66 (d, $J=9.6$ Hz, 1H), 4.37 (q, $J=6.8$ Hz, 2H), 1.62 (t, $J=6.8$ Hz, 3H). ^{13}C NMR (100 M, CDCl_3) δ 183.91, 162.82, 137.52, 136.17, 133.37, 132.47, 131.79, 128.70, 127.50, 127.38, 117.03, 115.83, 115.26, 65.47, 14.83. HRMS (ESI-FTMS) m/z found 303.0023 and 305.0003 ($\text{C}_{15}\text{H}_{12}\text{BrO}_2^+ [\text{M}+\text{H}]^+$, calcd: $m/z=303.0021$ and 305.0000).

4.2.2. 5-Bromo-9-(2-ethylhexoxy)-1-oxophenalene (7). 5-Bromo-9-hydroxy-1-oxophenalene (**6**) (5.48 g, 20 mmol), silver oxide (4.63 g, 20 mmol), and 2-ethylhexyl iodide (7.20 g, 30 mmol) were stirred in chloroform (50 mL). The mixture was held at reflux for 12 h, then cooled to room temperature and filtered. The filtrate was evaporated to dryness under reduced pressure. The crude product was chromatographed on silica gel using a mixture of petroleum ether and acetic ether as eluant (10: 1) to afford a yellow oil (5.51 g, yield 71%). ^1H NMR (400 M, CDCl_3): δ 8.02 (d, $J=9.2$ Hz, 1H), 8.01 (s, 1H), 7.78 (s, 1H), 7.55 (d, $J=9.6$ Hz, 1H), 7.46 (d, $J=9.2$ Hz, 1H), 6.71 (d, $J=9.6$ Hz, 1H), 4.21 (m, 2H), 1.95 (m, 1H), 1.80–1.50 (m, 4H), 1.36 (m, 4H), 0.98 (t, 3H), 0.91 (m, 3H). ^{13}C NMR (100 M, CDCl_3) δ 183.51, 163.06, 137.22, 136.02, 133.13, 132.30, 131.74, 128.58, 127.42, 127.20, 116.80, 115.76, 115.16, 72.05, 39.34, 30.14, 29.04, 23.55, 23.02, 14.17, 11.12. HRMS (ESI-FTMS) m/z found 409.0768 and 411.0750 ($\text{C}_{21}\text{H}_{23}\text{BrNaO}_2^+ [\text{M}+\text{Na}]^+$, calcd: 409.0779 and 411.0759).

4.2.3. 5,5',5''-(1,3,5-Phenylene)tris[9-(2-ethylhexoxy)-1-oxophenalene] (8). 5-Bromo-9-(2-ethylhexoxy)-1-oxophenalene (**7**) (186 mg, 0.48 mmol), 2-(3,5-bis(5,5-dimethyl-1,3,2-dioxaborinan-2-yl)phenyl)-5,5-dimethyl-1,3,2-dioxaborinane (**5**) (58 mg, 0.14 mmol), $\text{Pd}(\text{PPh}_3)_4$ (0.20 mg, 0.017 mmol), and NaHCO_3 (100 mg, 1.2 mmol) were stirred in the mixture of THF (18 mL) and H_2O (9 mL), under Ar atmosphere. After reflux for 8 h, the mixture were cooled to room temperature. The aqueous mixture was extracted with acetic ether for three times. The organic extracts were dried over MgSO_4 and taken down on a rotary evaporator to give a yellow solid and then purified by recrystallization from acetonitrile to give golden plates (71 mg, yield 51%). ^1H NMR (300 M, CDCl_3) δ 8.27 (s, 3H), 8.22 (d, $J=9.2$, 3H), 8.15 (s, 3H), 8.05 (s, 3H), 7.76 (d, $J=9.6$, 3H), 7.51 (d, $J=9.2$, 3H), 6.80 (d, $J=9.6$,

3H), 4.24 (m, 3H), 2.05–1.90 (m, 3H), 1.85–1.50 (m, 12H), 1.45–1.30 (m, 12H), 1.05–0.85 (m, 18H). ^{13}C NMR (100 M, CDCl_3) δ 184.15, 163.53, 141.37, 138.63, 137.48, 136.01, 131.48, 130.43, 129.13, 128.64, 127.87, 126.84, 125.13, 115.57, 115.53, 72.30, 39.40, 30.19, 29.07, 23.58, 23.03, 14.15, 11.07. HRMS (MALDI-FTMS) m/z found 1019.5227 ($\text{C}_{69}\text{H}_{72}\text{NaO}_6^+ [\text{M}+\text{Na}]^+$ calcd: 1019.5227).

4.2.4. 5,5',5''-(1,3,5-Phenylene)tris[1,9-dithiophenalenylium chloride] ($2^{3+}3\text{Cl}^-$). P_2S_5 (667 mg, 3 mmol), sublimed sulfur (6 mg, 0.2 mmol), and hexamethyldisiloxane (49 mg, 0.3 mmol) were stirred in toluene (150 mL) at room temperature for 10 min. Then 5,5',5''-(1,3,5-phenylene)tris[9-(2-ethylhexoxy)-1-oxophenalene] (**8**) (400 mg, 0.4 mmol) dissolved in 1,2-dichlorobenzene (50 mL) was added. The mixture were held at 85 °C overnight under Ar, then cooled to room temperature and filtered. Brown-black solid was obtained and washed twice using toluene. Then the brown-black solid was added to 4 M HCl (50 mL) and reflux 2 h under Ar. After cool to room temperature, the mixture was filtered, the solid was washed using distilled water, acetone, and methylene chloride. After vacuum dryness, brown solid was formed (507 mg). Without further treatment, the solid was used directly next step.

4.2.5. 5,5',5''-(1,3,5-Phenylene)tris[1,9-Dithiophenalenylium tetrakis[(3,5-trifluoromethyl)phenyl] borate] ($2^{3+}3\text{TFPB}^-$). Compound $2^{3+}3\text{Cl}^-$ (507 mg) and sodium tetrakis[3,5-bis(trifluoromethyl)phenyl]borate (**NaTFPB**) (1.44 g, 1.6 mmol) were stirred in dry methylene chloride under Ar at room temperature for 10 h. Filtered and solid was washed twice using methylene chloride. The filtrate was evaporated to dryness under reduced pressure to give a brown solid, which was purified by recrystallization from methylene chloride under -60 °C. After the impurity was filtered, the filtrate was evaporated to give a golden solid (896 mg, yield 62%). ^1H NMR (300 M, CD_3COCD_3) δ 9.89 (s, 2H), 9.44 (d, $J=9.0$, 2H), 9.30 (d, $J=9.0$, 2H), 9.11 (s, 1H), 7.78 (m, 8H), 7.67 (s, 4H). ^{13}C NMR (100 M, CD_3COCD_3) δ 168.65, 162.62 (q), 143.43, 142.64, 141.24, 135.56, 130.80, 130.27, 129.81, 129.48, 127.20, 125.37, 123.60, 119.99, 118.45. HRMS (MALDI-FTMS) m/z 752.9965 ($\text{C}_{45}\text{H}_{21}\text{S}_6 [\text{M}]^+$ calcd: $m/z=752.9967$).

Acknowledgements

The authors gratefully acknowledge financial support from the NSFC (Grants 50933003, 21004043 and 51273093), MOST (Grants 2012CB933401 and 2011DFB50300) and NSF of Tianjin City (Grant 10ZCGHHZ00600).

Supplementary data

^1H NMR, ^{13}C NMR, and MS for compounds of **3**, **7** and $2^{3+}3\text{TFPB}^-$. Solubility of 2^{3+} salt with different anions and other information. Supplementary data associated with this article can be found in the online version, at <http://dx.doi.org/10.1016/j.tet.2013.05.111>. These data include MOL files and InChIKeys of the most important compounds described in this article.

References and notes

- [1] Z. Sun, Q. Ye, C. Chi, J. Wu, Chem. Soc. Rev. 41 (2012) 7857.
- [2] Y. Morita, S. Suzuki, K. Sato, T. Takui, Nat. Chem. 3 (2011) 197.
- [3] R.C. Haddon, Nature 256 (1975) 394.
- [4] R.C. Haddon, Aust. J. Chem. 28 (1975) 2343.
- [5] P. Bag, M.E. Itkis, S.K. Pal, B. Donnadieu, F.S. Tham, H. Park, J.A. Schlueter, T. Siegrist, R.C. Haddon, J. Am. Chem. Soc. 132 (2010) 2684.
- [6] T. Kubo, Y. Katada, A. Shimizu, Y. Hirao, K. Sato, T. Takui, M. Uruichi, K. Yakushi, R.C. Haddon, J. Am. Chem. Soc. 133 (2011) 14240.
- [7] S.K. Pal, M.E. Itkis, F.S. Tham, R.W. Reed, R.T. Oakley, R.C. Haddon, J. Am. Chem. Soc. 130 (2008) 3942.
- [8] S.K. Pal, M.E. Itkis, F.S. Tham, R.W. Reed, R.T. Oakley, B. Donnadieu, R.C. Haddon, J. Am. Chem. Soc. 129 (2007) 7163.

- [9] P.A. Koutentis, Y. Chen, Y. Cao, T.P. Best, M.E. Itkis, L. Beer, R.T. Oakley, A.W. Cordes, C.P. Brock, R.C. Haddon, *J. Am. Chem. Soc.* 123 (2001) 3864.
- [10] L. Beer, S.K. Mandal, R.W. Reed, R.T. Oakley, F.S. Tham, B. Donnadiou, R.C. Haddon, *Cryst. Growth Des.* 7 (2007) 802.
- [11] L. Beer, R.W. Reed, C.M. Robertson, R.T. Oakley, F.S. Tham, R.C. Haddon, *Org. Lett.* 10 (2008) 3121.
- [12] A. Sarkar, S.K. Pal, M.E. Itkis, F.S. Tham, R.C. Haddon, *J. Mater. Chem.* 22 (2012) 8245.
- [13] A. Sarkar, F.S. Tham, R.C. Haddon, *J. Mater. Chem.* 21 (2011) 1574.
- [14] K. Goto, T. Kubo, K. Yamamoto, K. Nakasuji, K. Sato, D. Shiomi, T. Takui, M. Kubota, T. Kobayashi, K. Yakusi, J. Ouyang, *J. Am. Chem. Soc.* 121 (1999) 1619.
- [15] Y. Morita, T. Aoki, K. Fukui, S. Nakazawa, K. Tamaki, S. Suzuki, A. Fuyuhiko, K. Yamamoto, K. Sato, D. Shiomi, A. Naito, T. Takui, K. Nakasuji, *Angew. Chem., Int. Ed.* 41 (2002) 1793.
- [16] Y. Morita, T. Ohba, N. Haneda, S. Maki, J. Kawai, K. Hatanaka, K. Sato, D. Shiomi, T. Takui, K. Nakasuji, *J. Am. Chem. Soc.* 122 (2000) 4825.
- [17] Y. Hou, H. Wang, Z. Li, Y. Liu, X. Wan, X. Xue, Y. Chen, A. Yu, *Tetrahedron Lett.* 52 (2011) 3670.
- [18] K. Nakasuji, K. Yoshida, I. Murata, *J. Am. Chem. Soc.* 104 (1982) 1432.
- [19] K. Ohashi, T. Kubo, T. Masui, K. Yamamoto, K. Nakasuji, T. Takui, Y. Kai, I. Murata, *J. Am. Chem. Soc.* 120 (1998) 2018.
- [20] P. Bag, F.S. Tham, B. Donnadiou, R.C. Haddon, *Org. Lett.* 15 (2013) 1198.
- [21] L. Zhang, S.M. Fakhouri, F. Liu, J.C. Timmons, N.A. Ran, A.L. Briseno, *J. Mater. Chem.* 21 (2011) 1329.
- [22] T. Mochida, S. Suzuki, I. Takasu, T. Sugawara, *J. Phys. Chem. Solids* 64 (2003) 1257.
- [23] X. Chi, M.E. Itkis, B.O. Patrick, T.M. Barclay, R.W. Reed, R.T. Oakley, A.W. Cordes, R.C. Haddon, *J. Am. Chem. Soc.* 121 (1999) 10395.
- [24] X. Chi, M.E. Itkis, R.W. Reed, R.T. Oakley, A.W. Cordes, R.C. Haddon, *J. Phys. Chem. B* 106 (2002) 8278.
- [25] S.K. Pal, M.E. Itkis, R.W. Reed, R.T. Oakley, A.W. Cordes, F.S. Tham, T. Siegrist, R. C. Haddon, *J. Am. Chem. Soc.* 126 (2004) 1478.
- [26] S.K. Mandal, M.E. Itkis, X. Chi, S. Samanta, D. Lidsky, R.W. Reed, R.T. Oakley, F.S. Tham, R.C. Haddon, *J. Am. Chem. Soc.* 127 (2005) 8185.
- [27] S.K. Mandal, S. Samanta, M.E. Itkis, D.W. Jensen, R.W. Reed, R.T. Oakley, F.S. Tham, B. Donnadiou, R.C. Haddon, *J. Am. Chem. Soc.* 128 (2006) 1982.
- [28] A. Sarkar, S.K. Pal, M.E. Itkis, P. Liao, F.S. Tham, B. Donnadiou, R.C. Haddon, *Chem. Mater.* 21 (2009) 2226.
- [29] Y. Li, W.-K. Heng, B.S. Lee, N. Aratani, J.L. Zafra, N. Bao, R. Lee, Y.M. Sung, Z. Sun, K.-W. Huang, R.D. Webster, J.T. López Navarrete, D. Kim, A. Osuka, J. Casado, J. Ding, J. Wu, *J. Am. Chem. Soc.* 134 (2012) 14913.
- [30] Z. Sun, J. Wu, *J. Mater. Chem.* 22 (2012) 4151.
- [31] L. Pisani, J.A. Chan, B. Montanari, N.M. Harrison, *Phys. Rev. B* 75 (2007) 064418.
- [32] Y. Wang, Y. Huang, Y. Song, X. Zhang, Y. Ma, J. Liang, Y. Chen, *Nano. Lett.* 9 (2008) 220.
- [33] G. Ning, C. Xu, L. Hao, O. Kazakova, Z. Fan, H. Wang, K. Wang, J. Gao, W. Qian, F. Wei, *Carbon* 51 (2013) 390.
- [34] J. Fernández-Rossier, J.J. Palacios, *Phys. Rev. Lett.* 99 (2007) 177204.
- [35] J. Bai, R. Cheng, F. Xiu, L. Liao, M. Wang, A. Shailos, K.L. Wang, Y. Huang, X. Duan, *Nat. Nanotechnol.* 5 (2010) 655.
- [36] S.M. Winter, S. Datta, S. Hill, R.T. Oakley, *J. Am. Chem. Soc.* 133 (2011) 8126.
- [37] Y.W. Ma, Y.H. Lu, J.B. Yi, Y.P. Feng, T.S. Herng, X. Liu, D.Q. Gao, D.S. Xue, J.M. Xue, J.Y. Ouyang, J. Ding, *Nat. Commun.* 3 (2012) 727.
- [38] J.S. Miller, *Chem. Soc. Rev.* 40 (2011) 3266.
- [39] J. Fujita, M. Tanaka, H. Suemune, N. Koga, K. Matsuda, H. Iwamura, *J. Am. Chem. Soc.* 118 (1996) 9347.
- [40] H. Nishide, R. Doi, K. Oyaizu, E. Tsuchida, *J. Org. Chem.* 66 (2001) 1680.
- [41] R.C. Haddon, F. Wudl, M.L. Kaplan, J.H. Marshall, R.E. Cais, F.B. Bramwell, *J. Am. Chem. Soc.* 100 (1978) 7629.
- [42] W. Yan, X. Wan, Y. Xu, X. Lv, Y. Chen, *Synth. Met.* 159 (2009) 1772.
- [43] J.C. Thomas, *Tetrahedron Lett.* 41 (2000) 9963.
- [44] J.C. Thomas, *Tetrahedron Lett.* 43 (2002) 371.
- [45] T. Ozturk, E. Ertas, O. Mert, *Chem. Rev.* 107 (2007) 5210.
- [46] Gaussian 09, Revision B.01, Gaussian, Wallingford CT, 2010, 2010. See Supporting information for full citation.
- [47] T. Mochida, A. Izuoka, T. Sugawara, Y. Moritomo, Y. Tokura, *J. Chem. Phys.* 101 (1994) 7971.
- [48] N.A. Yakelis, R.G. Bergman, *Organometallics* 24 (2005) 3579.
- [49] R.W. Tilford, W.R. Gemmill, H.-C. zur Loye, J. Lavigne, *J. Chem. Mater.* 18 (2006) 5296.